Journal of Power Sources 272 (2014) 160–168

Contents lists available at ScienceDirect

Journal of Power Sources

journal homepage: www.elsevier.com/locate/jpowsour

Energy management of power-split plug-in hybrid electric vehicles based on simulated annealing and Pontryagin's minimum principle

Zheng Chen, Chunting Chris Mi*, Bing Xia, Chenwen You

University of Michigan-Dearborn, United States

HIGHLIGHTS

- Use quadratic equations to calculate fuel rate as a function of battery current.
- Use SA and PMP to determine engine-on power and battery current.
- Fuel economy is improved, as validated by simulation.
- Battery state of health is introduced to extend the application.

ARTICLE INFO

Article history:
Received 8 January 2014
Received in revised form
9 August 2014
Accepted 14 August 2014
Available online 27 August 2014

Keywords:
Plug-in hybrid electric vehicles
Fuel-rate
Pontryagin's minimum principle
Simulated annealing
State of health

ABSTRACT

In this paper, an energy management method is proposed for a power-split plug-in hybrid electric vehicle (PHEV). Through analyzing the PHEV powertrain, a series of quadratic equations are employed to approximate the vehicle's fuel-rate, using battery current as the input. Pontryagin's Minimum Principle (PMP) is introduced to find the battery current commands by solving the Hamiltonian function. Simulated Annealing (SA) algorithm is applied to calculate the engine-on power and the maximum current coefficient. Moreover, the battery state of health (SOH) is introduced to extend the application of the proposed algorithm. Simulation results verified that the proposed algorithm can reduce fuel-consumption compared to charge-depleting (CD) and charge-sustaining (CS) mode.

1. Introduction

Nowadays, plug-in hybrid electric vehicles (PHEVs) have accounted for a growing share of the vehicle market as they combine the merits of electric vehicles (EVs) and conventional hybrid electric vehicles (HEVs) to save fossil fuel and reduce emissions. PHEVs are usually equipped with an internal combustion engine (ICE) and one or two electric motors that can be driven by an electric energy storage system, such as a battery system [1–4]. Since the ICE and the motor can each drive the vehicle, it becomes essential to control the energy distribution between the battery system and the ICE to improve the vehicle's performance without influencing its drivability. A good energy management strategy can effectively improve fuel economy, prolong battery life, and decrease emissions. For a PHEV, the most direct and easiest way to realize the energy management is to separate the vehicle running modes into two basic modes: pure electric driving mode and hybrid driving mode. During the pure electric driving mode, the vehicle is only powered by the battery until its state of charge (SoC) decreases to a preset critical value [5]. This process is also called charge-depleting (CD) mode. During the hybrid driving mode, the vehicle is powered by the ICE and the battery together to maintain the battery SoC in the neighborhood of a preset critical value. This mode is also called charge-sustaining (CS) mode [6].

Many studies have been carried out to improve the energy management for HEVs or PHEVs. Provided that the strategies do not impact driving performance, the targets usually include improving fuel economy [7–10], prolonging battery life [11], decreasing emissions [12], or both [1,11,13]. A variety of intelligent methods, such as fuzzy logic [8,14], neural network [15–17], genetic algorithm [18], model predictive control [19], and sliding

* Corresponding author. Tel.: +1 313 583 6434.
E-mail addresses: chrismi@umich.edu, mi@ieee.org (C.C. Mi).

http://dx.doi.org/10.1016/j.jpowsour.2014.08.057
0378-7753/

mode control [1,13], have been successfully applied to realize the energy management. These methods try to locate engine and motor operation in the high efficiency region. In addition, analytical methods and rule-based methods [20,21] are also employed to improve the fuel economy of PHEVs. In Ref. [20], by analyzing the electric driveline loss and modeling the fuel consumption, the energy management algorithm is represented by a pair of parameters that describe the engine-on power threshold and the battery optimal power.

Optimal theories are also competitive candidates for managing the energy distributions of HEVs and PHEVs. Given the trip information, dynamic programming (DP) [8,9,15,16,22,23] can find an optimal solution to reduce fuel-consumption in a HEV or PHEV. However, DP suffers from considerable computation time, which limits its online application. A two-scale DP approach [24] was applied to decrease calculation time to some degree. This method splits the whole trip into a number of segments, and applies DP twice during the whole trip and each segment for improving the energy management. In Ref. [18,25], the quadratic programming (QP) method was applied to the energy management of PHEV. This method, which depicts engine fuel-rate as multiple quadratic equations with respect to battery currents at different driveline powers and vehicle speeds, needs to determine engine-on power based on other intelligent methods [18]. This is time-consuming, since GA needs a series of actions including crossover, mutation, and selection in order to find the optimal solution. Pontryagin's minimum principle (PMP) [11,26–28] is another alternative to realize the optimal energy management based on a precise powertrain model. In Ref. [26], PMP was applied for the energy management of a hybrid electric truck, whose battery SoC is sustained within a small variation range. In Ref. [27], a comparison of DP and PMP for energy management of a hybrid electric truck was studied, which shows that their results are almost the same, but PMP computes faster than the DP method. However, in this case, the target is a conventional HEV, while the algorithm for PHEV is more complex.

Upon analysis of the mentioned references, it proves essential to build an effective controller to improve the energy management for a PHEV that has a fast calculation speed. In this paper, a power-split PHEV is selected as the research object with the target of improving the fuel economy over a certain trip. More running modes exist in a power-split PHEV than in a series or a parallel PHEV. Therefore, the algorithm developed in this paper can also be applicable for other types of PHEVs.

Many vehicles today are equipped with a Global Positioning System (GPS) [2,29], geographic information system (GIS) [30], or online communication services, such as OnStar systems [31]. All of these can provide detailed trip information, including speed profile and road declivity. Based on this information, the vehicle driveline power can be properly estimated. Then, according to the speed profile, road declivity, and the calculated driveline power, a series of quadratic equations can be introduced to build the relationship between fuel-rate and battery current. Furthermore, PMP and simulated annealing (SA) [32,33] algorithm are introduced to determine the control commands and to optimize the engine-on power. A battery management system (BMS) [11,34] can easily provide the battery SoC and battery state of health (SoH), which can reflect the available battery capacity and can influence the energy management strategy. When the battery becomes unhealthy, the battery open-circuit voltage (OCV) will drop and the internal resistance will increase. Thus, the efficiency of an unhealthy battery becomes lower compared to the efficiency of a healthy battery [32]. The proposed algorithm considers the battery SoH to extend its applicability. Simulation results verified that the proposed algorithm is effective in reducing fuel-consumption with fast calculation speed.

2. Vehicle driveline analysis and simplification

The objective of this paper is to minimize the fuel-consumption of a power-split PHEV, as shown in (1).

$$\min F = \min \int_0^{\text{t\_total}} m_{\text{f}}(t)dt \tag{1}$$

$$m_{\text{f}} = f(w_{\text{eng}}, T_{\text{eng}}, \text{eng\_on}) \tag{2}$$

where F is the total fuel-consumption, t_total is the trip duration, m_{f} denotes the fuel-rate, and f is a highly nonlinear function calculating m_{f} based on engine torque T_{eng}, engine speed w_{eng}, and engine on/off status eng_on.

In order to minimize F, the vehicle driveline is analyzed to determine the variables that influence m_{f}. The parameters of the analyzed vehicle are listed in Table 1. It has a lithium-ion battery pack of 20 Ah. Fig. 1 shows the driveline of the analyzed PHEV, which consists of a power split device, i.e., a planetary gear set, an engine, and two electric motors. Fig. 2 shows the lever analogy of the driveline analyzed in the paper. As shown in Fig. 2, the driveline has two independent control variables. Given the driveline torque and vehicle speed, any two torques or speeds depicted in Fig. 2 can determine the remaining variables. For speed and torque response, there exist two basic equations,

$$\begin{cases} (1+\rho)\cdot w_{\text{eng}} = \rho \cdot w_{\text{mot2}} + w_{\text{r}} \\ T_{\text{eng}} = (1+1/\rho)\cdot T_{\text{mot2}} = (1+\rho)\cdot T_{\text{r}} \end{cases} \tag{3}$$

where ρ is the ratio between the ring gear and sun gear.

Based on (2) and (3), in order to calculate the fuel-rate, the engine torque and speed should be respectively determined based on the speed and torque of the two motors [18,19]. The battery power (current) can then be obtained accordingly. It is complicated to calculate the fuel rate directly with the battery power/current as the input. Here, an alternate method is proposed to determine the fuel rate. As can be seen from Figs. 1 and 2, the driveline is a system with two degrees-of-freedom, which considerably complicates the task of realizing optimal control. Based on (3), the torque and speed of the ring gear (Motor 1) or Motor 2 can regulate the engine torque and speed. Here, a method is introduced to simplify the degrees-of-freedom of the problem from two to one [18,29]. For different engine operating powers, the combinations of speeds and torques that will maximize efficiency of the engine can be determined. This means that for a certain power output, the engine can only work with

Table 1
Vehicle specifications.

Type	Power-split plug-in HEV
Vehicle	Front-wheel drive Mass 1641.3 kg
Engine	Rated power 57 kW
Motor 1	Rated power 25 kW Peak power 50 kW
Power converter 1	Average efficiency 95% Peak power 55 kW
Motor 2	Rated power 15 kW Peak power 30 kW
Power converter 2	Average efficiency 95% Peak power 33 kW
Planetary gear set	Ring gear 78 Sun gear 30
Battery	Lithium-ion battery pack Rated voltage 340 V Rated capacity 20 Ah

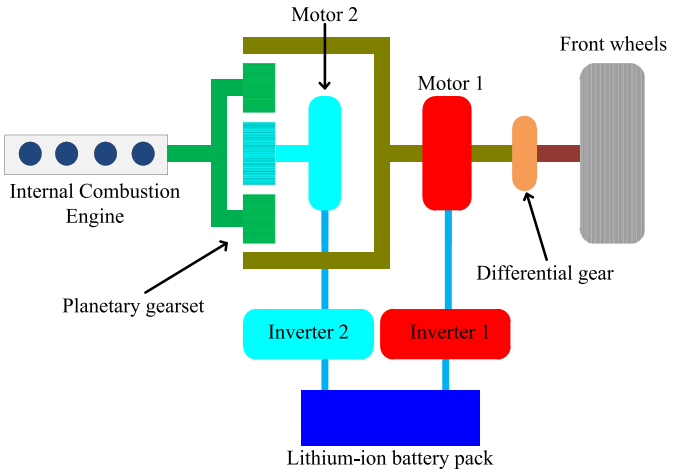

Fig. 1. The analyzed vehicle driveline structure.

a predetermined speed and torque output. Thus, the engine always works in the optimal efficiency region. The optimal engine speed profile based on the proposed method is shown in Fig. 3. Through this method, only one variable can determine the fuel-rate within the constraints of each component, such as the maximum current of the battery, as well as the maximum power and speed of the motors and the engine. In this paper, the battery current is adopted as the control variable to optimize the fuel-rate, as shown in (4),

$$m_f = f\left(I, P_o, w_o, \text{eng\_on}\right) \tag{4}$$

where I is the battery current, P_o is the driveline power, and w_o is the driveline speed.

To simplify the calculation without sacrificing precision, a series of quadratic equations are introduced to approximate the fuel-rate when the engine is on,

$$m_f = \varphi_2(w_o, P_o)\cdot I^2 + \varphi_1(w_o, P_o)\cdot I + \varphi_0(w_o, P_o) \tag{5}$$

where $\varphi_2(w_o, P_o)$, $\varphi_1(w_o, P_o)$, and $\varphi_0(w_o, P_o)$ are coefficients changing with P_o and w_o. It is necessary to mention that the average OCV and average internal resistance of the battery are adopted to obtain these coefficients. Here, the maximum speed of the vehicle is 38 m s^{-1} and the maximum driveline power is 57 kW. The increment of vehicle speed and the increment of driveline power to

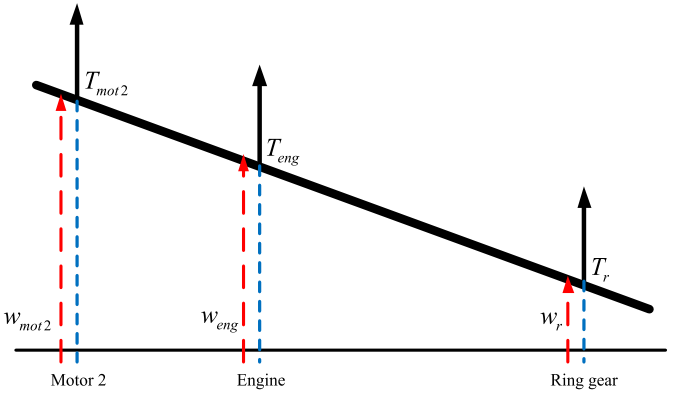

Fig. 2. The lever analogy of the driveline analyzed in the paper, where w_r, w_{mot2}, and w_{mot1} denote speeds of the driving axle, Motor 2, and Motor 1, and T_r, T_{mot2}, and T_{mot1} are the torques of the ring gear, Motor 1, and Motor 2.

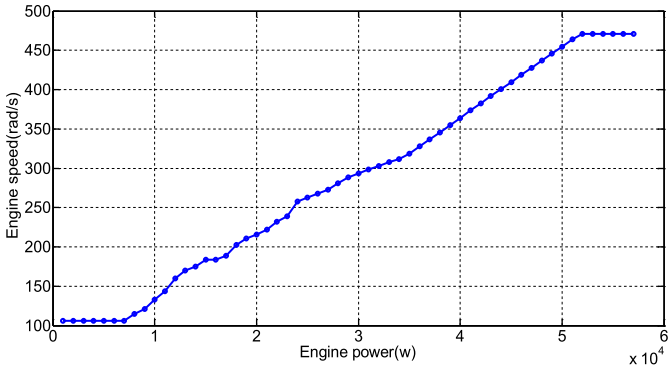

Fig. 3. The optimal engine speed profile at different powers.

obtain the coefficients using the curve fitting method are 0.5 m s^{-1} and 1 kW, respectively. Therefore, the dimensions of $\varphi_2(w_o, P_o)$, $\varphi_1(w_o, P_o)$, and $\varphi_0(w_o, P_o)$ are 76 by 57. Fig. 4 presents $\varphi_2(w_o, P_o)$, which is always more than zero at any vehicle speed and driveline power. Fig. 5 compares the simulated fuel-rate and the fuel-rate calculated by the quadratic equations. It is observed that the quadratic equations can effectively approximate the fuel-rate.

From (5), there exists only one input, i.e. battery current, to calculate the fuel-rate, thus making it easier to realize the energy management. In the next step, PMP can be introduced to find the optimal solution to reduce the fuel-consumption.

3. PMP analysis and application

PMP is an optimal theory that can be employed to find the best solution for a dynamic control system, especially when the system is constrained by states or inputs. It states that, through minimization of Hamiltonian function, the possible best control solution can easily be found [12,27,28]. In order to build the Hamiltonian function, the fuel-rate should be analyzed further. Based on (4) and (5), we can calculate

$$\dot{x}_1 = [2\varphi_2(w_o, P_o)\cdot u_1 + \varphi_1(w_o, P_o)]\cdot u_2 \tag{6}$$

where x_1 is the fuel-rate, u_1 is the battery current, and u_2 is the engine on/off command, which equals 1 when the engine is on. Moreover, the battery SoC can also be calculated,

$$\dot{x}_2(t) = k\cdot u_1(t) \tag{7}$$

where x_2 denotes the battery SoC, and k is a constant determined by the battery capacity. In this paper, the battery SoC is limited within [0.2, 1], and the final SoC when the trip ends should be 30%.

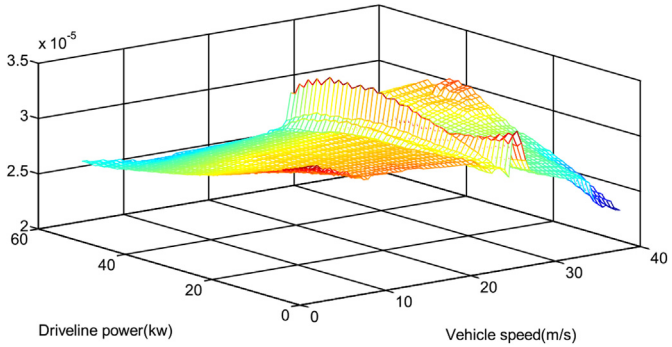

Fig. 4. The value of $\varphi_2(w, P_o)$.

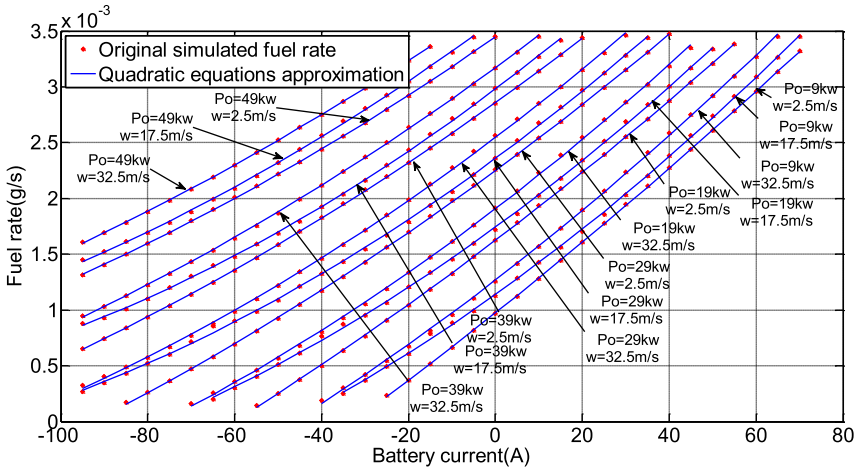

Fig. 5. Fuel-rate approximation.

For a given trip, the driveline power and the vehicle speed are different at each time step. Accordingly, there are different constraints for the battery current,

$$u_{1\min}(t) \le u_1(t) \le u_{1\max}(t) \tag{8}$$

where $u_{1\min}(t)$ is the minimum current that is determined when the vehicle is only powered by the battery, and $u_{1\max}(t)$ denotes the maximum charge current that is limited by the driveline power, the engine maximum power, and the maximum power of the electric motors. Since there is a constraint for x_2, in order to obtain the solution based on PMP, another variable x_3 is introduced,

$$\begin{aligned} H &= x_1(t)u_2(t) + \lambda_1(t)\dot{x}_1(t) + \lambda_2(t)\dot{x}_2(t) + \lambda_3(t)\dot{x}_3(t) \\ &= x_1(t)u_2(t) + \lambda_1(t)\left(2\varphi_2(t)\cdot u_1(t) + \varphi_1(t)\right)u_2(t) \\ &\quad + \lambda_2(t)ku_1(t) + \lambda_3(t)(x_2(t) - x_{2\min})^2 \cdot G(x_{2\min} - x_2(t)) \\ &\quad + \lambda_3(t)(x_{2\max} - x_2(t))^2 \cdot G(x_2(t) - x_{2\max}) \end{aligned} \tag{12}$$

where H is the Hamiltonian function, and $\lambda_1(t)$, $\lambda_2(t)$, and $\lambda_3(t)$ are three co-state variables.

Solve (12) to obtain the partial derivatives of $\lambda_1(t)$, $\lambda_2(t)$, and $\lambda_3(t)$,

$$\begin{cases} \dot{\lambda}_1^*(t) = -\dfrac{\partial H}{\partial x_1} = -u_2(t) \\ \dot{\lambda}_2^*(t) = -\dfrac{\partial H}{\partial x_2} = -2(x_2(t) - x_{2\min}) \times G(x_{2\min} - x_2(t)) + 2(x_{2\max} - x_2(t)) \times G(x_2(t) - x_{2\max}). \\ \dot{\lambda}_3^*(t) = -\dfrac{\partial H}{\partial x_3} = 0 \end{cases} \tag{13}$$

$$\begin{aligned} \dot{x}_3(t) &= (x_2(t) - x_{2\min})^2 \times G(x_{2\min} - x_2(t)) + (x_{2\max} - x_2(t))^2 \\ &\quad \times G\left(x_2(t) - x_{2\max}\right) \end{aligned} \tag{9}$$

where $x_{2\min}$ and $x_{2\max}$ equal 0.2 and 1, respectively. $G(\ )$ is a Heaviside step function:

$$G(x_{2\min} - x_2(t)) = \begin{cases} 0 & x_2(t) \ge 0.2 \\ 1 & x_2(t) < 0.2 \end{cases} \tag{10}$$

$$G(x_2(t) - x_{2\max}) = \begin{cases} 0 & x_2(t) \le 1 \\ 1 & x_2(t) > 1 \end{cases}. \tag{11}$$

Based on (6) to (9), PMP can be applied to optimize the fuel-consumption, and the Hamiltonian function can be formulated,

The beginning and cut-off conditions for each variable are

$$\begin{cases} x_1(t_0) = x_{10} & x_1(\text{t\_total}) = 0 \\ x_2(t_0) = \text{SoC}_0 & x_2(\text{t\_total}) = 0.3 \\ x_3(t_0) = 0 & x_3(\text{t\_total}) = 0 \end{cases} \tag{14}$$

where SoC_0 is the initial SoC value when the vehicle starts. Based on (6) to (13), the terminal values of three co-state variables can be calculated,

$$\begin{cases} \lambda_1^*(\text{t\_total}) = 0 \\ \lambda_2^*(\text{t\_total}) = \gamma_1 \\ \lambda_3^*(\text{t\_total}) = \gamma_2 \end{cases} \tag{15}$$

where γ_1 and γ_2 are constants. From (13), if $x_2(t)$ is within [0.2 1], then $\dot{\lambda}_2^*(t) = 0$. This means that if the SoC is within this range, it

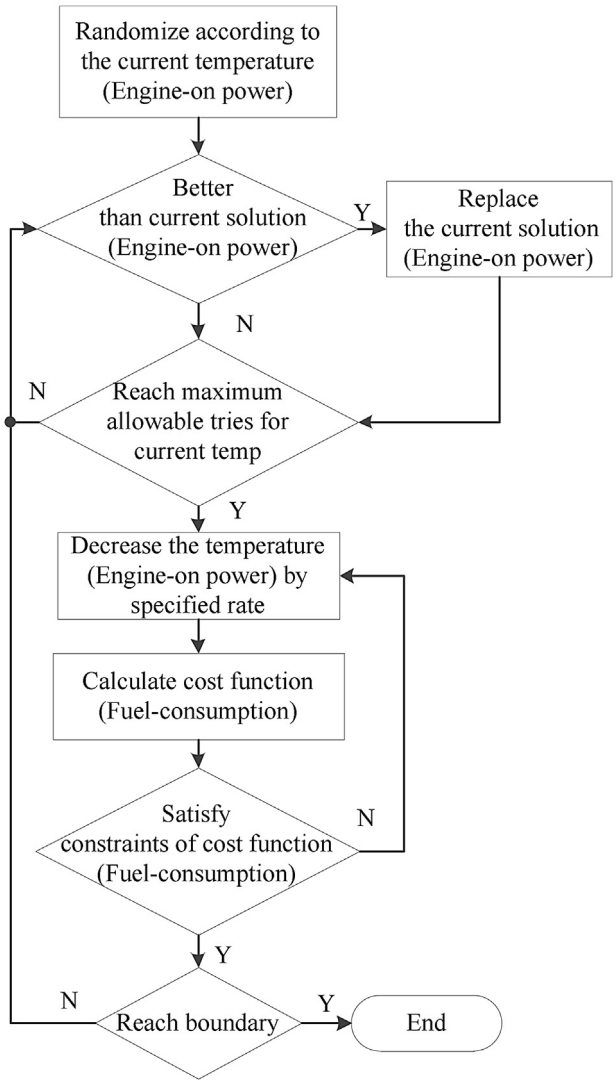

Fig. 6. The SA method calculating process.

should be a constant, and thus the co-state equation can be obtained,

$$\begin{aligned}\lambda_1^*(t) &= \sum_{t=0}^{\text{t\_total}} u_2(t) - t u_2(t)\\ \lambda_2^*(t) &= \gamma_1\\ \lambda_3^*(\text{t\_total}) &= \gamma_2.\end{aligned} \tag{16}$$

Based on (12), the solution can be easily obtained to minimize H,

$$u_1(t) = \begin{cases} u_{1\min}(t) & 2\lambda_1(t)\varphi_2(t) + \lambda_2(t)k \geq 0 \\ u_{1\max}(t) & 2\lambda_1(t)\varphi_2(t) + \lambda_2(t)k < 0 \end{cases}. \tag{17}$$

In this way, the solution of current commands that depend on $\lambda_1(t)$, $\lambda_2(t)$, and $\varphi_2(t)$ can be obtained. From (16), $\lambda_2^*(t)$ is a constant, and $\lambda_1^*(t)$ decreases gradually. This means that the engine is off during the first part of the trip and on during the latter half of the trip. During the first part of the trip, the vehicle is only driven by the battery, while during the latter part, the engine is always on and outputs the maximum power to charge the battery. However, a problem arises when the battery is discharged and then charged again to the SoC of 30%. The battery SoC can easily drop below 20%; therefore, this solution cannot meet the assumption in (16). From (17), the solution should be a mixture of $u_{\min}(t)$ and $u_{\max}(t)$. Now a proper sequence of $u_{\min}(t)$ and $u_{\max}(t)$ should be arranged to ensure the SoC varies between 20% and 100%. Meanwhile, the maximum value of battery current at each step can be reconsidered. Here, two coefficients α and β are introduced to formulate an updated solution,

$$u_1(t) = \begin{cases} u_{1\min}(t) & P_o \leq \alpha \\ \beta u_{1\max}(t) & P_o > \alpha \end{cases} \tag{18}$$

where α is the engine-on power, and β is the maximum current coefficient that is within [0, 1]. When P_o is not more than α, the battery current value is $u_{\min}(t)$ and the engine is off. When P_o is more than α, the battery current command is $\beta u_{\max}(t)$ and the engine is on.

It is difficult to find the optimal α and β, as the fuel-rate, which is expressed by a series of quadratic equations, relies on the random driving conditions. In the next section, the SA method is applied to find these coefficients.

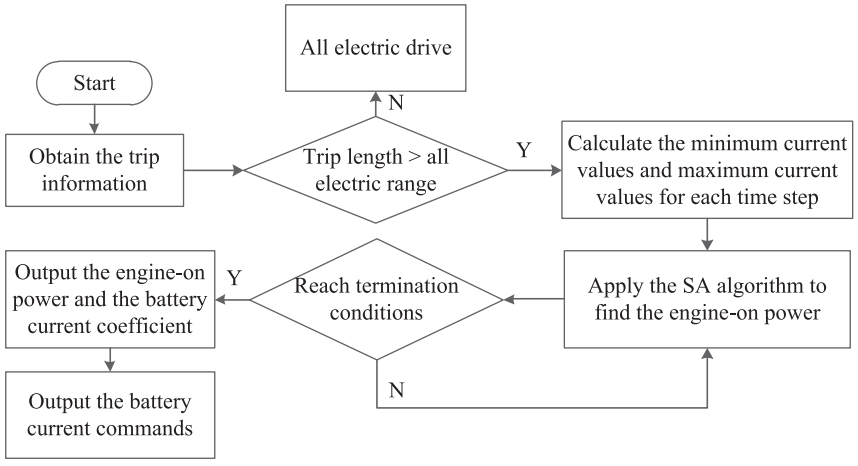

Fig. 7. The whole application process.

4. Simulated annealing method and its application

The SA method is a generic method to locate a quasi-optimal solution for a given global optimization problem. It is more efficient than an exhaustive method or some deterministic method such as DP, provided that the goal is only to find a good solution rather than the best possible solution [32,33,35,36]. The proposed energy management problem is highly nonlinear, making it difficult to find the optimal control coefficients through analytical or numeric methods. The SA method is introduced to find them effectively.

The inspiration for the SA method comes from the annealing process of metal, in which the sizes of crystals are increased through the heating and cooling of the material. As shown in Fig. 6, the SA method selects the engine-on power α as the control target, with the fuel-consumption as the output. Meanwhile, the maximum current coefficient β is calculated by satisfying the constraints of driving power and the battery SoC. The SA method usually sets a high value for α, then gradually decreases this value based on the result comparison when different inputs are considered. The interval between the updated and current values of α is subject to a probability distribution. During the iteration, the optimal cost function output, i.e., the calculated fuel-consumption, and the corresponding α are updated and recorded at all times. When the termination conditions are satisfied, the algorithm will stop and finally output the optimal α and β. Generally, the SA method adopts the following conditions to determine when to stop the iteration:

- Finding a solution that satisfies the set criteria
- Reaching the maximum setting iterations

In this paper, the maximum iteration of the SA method is 100, the initial engine-on power is 30 kW, and the termination tolerance on function value is 0.005. The whole application process is shown in Fig. 7. If the trip length is less than the all-electric range (AER), which can be calculated based on battery current SoC and trip information, the vehicle is only powered by the battery. If the trip length is more than the calculated AER, the maximum and minimum current values at each step can be calculated, after which the SA method will be implemented to obtain the engine-on power α and the maximum current coefficient β. Finally, the engine-on power and the current commands, which combine the minimum and updated maximum current values, can be supplied to the vehicle controller. In the next step, simulations were conducted to show the calculation process and the control performance.

5. Simulation validation

In order to validate the algorithm, many simulations were carried out. All the simulations were realized based on Autonomie, which is a model-based powertrain and vehicle simulation software. Autonomie can effectively model a plant, synthesize and analyze a controller for the plant, simulate the plant and its controller, and program the controller [37,38]. From (7), k is related to battery capacity, which means that if we know the battery capacity in advance, the algorithm can still be applicable even when the battery capacity degrades. Therefore, the simulations were performed with both healthy and unhealthy batteries.

5.1. Simulation with a healthy battery

Highway Fuel Economy Test (HWFET) cycle and Environmental Protection Agency (EPA) Urban Dynamometer Driving Schedule (UDDS), which are shown in Fig. 8, were simulated to verify the proposed algorithm. The UDDS cycle, which simulates an urban route of 12.07 km with 19 stops, has a duration of 1369 s, a maximum speed of 91.2 km h^{-1}, and an average speed of 31.5 km h^{-1}. The HWFET cycle, which is used to determine the highway fuel economy rating with a total distance of 16.45 km and no stop, has a duration of 765 s, a maximum speed of 96.5 km h^{-1}, and an average speed of 77.7 km h^{-1}.

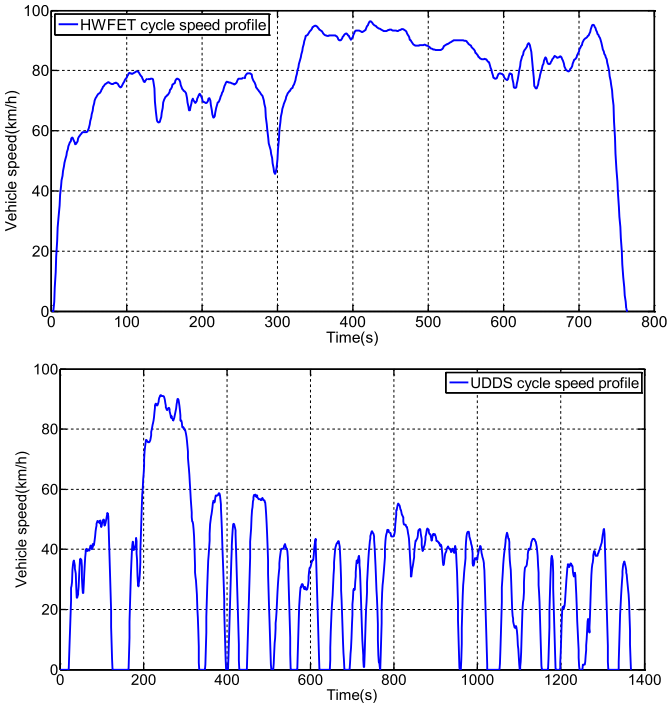

Fig. 8. The speed profiles of HWFET and UDDS drive cycles.

First, the CD/CS algorithm was employed to get a benchmark of the fuel-consumption. In this paper, the beginning battery SoC is

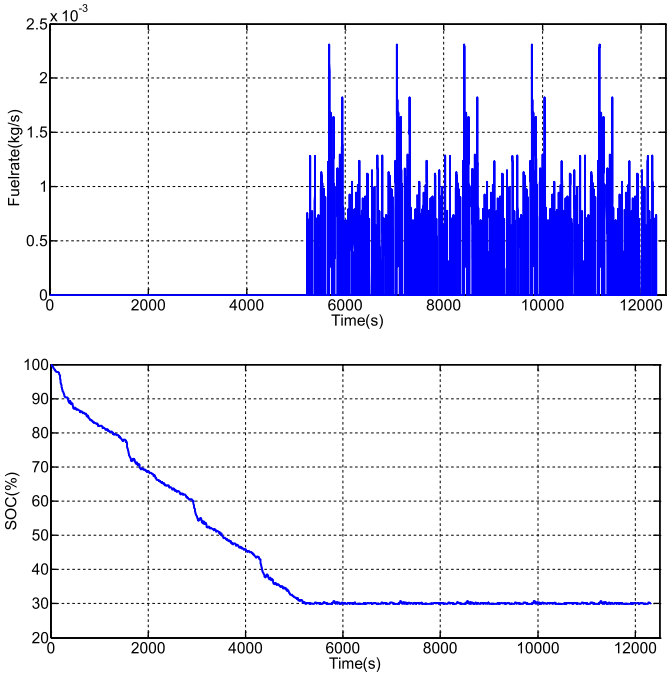

Fig. 9. Engine fuel-rate and battery SoC.

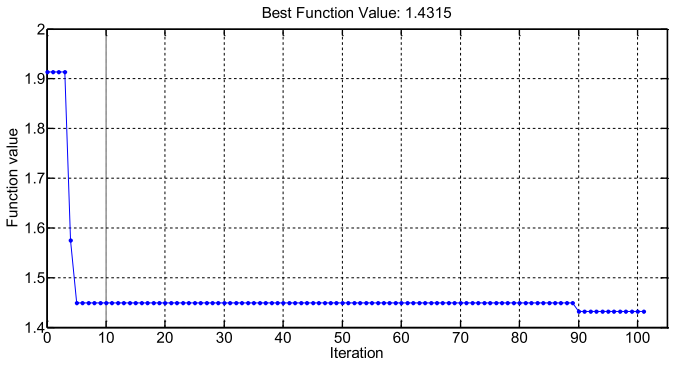

Fig. 10. The SA method calculation process.

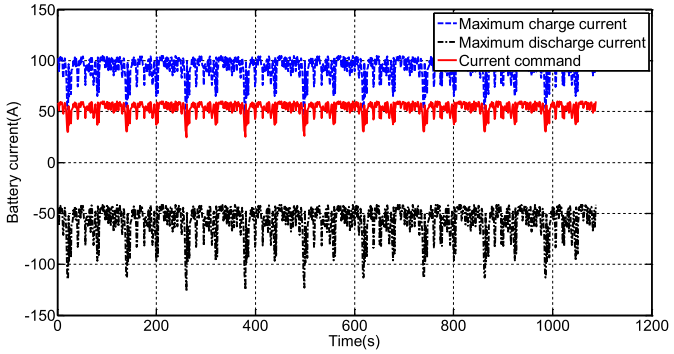

Fig. 11. The maximum current, minimum current, and current commands when the engine is on.

100%. Fig. 9 shows the fuel-rate and battery SoC variations when the vehicle was simulated with nine consecutive UDDS cycles. It is observed that the engine is off until 5300 s, after which the engine is turned on to power the vehicle.

The proposed method is applied to verify its performance. Fig. 10 shows the calculation process of the SA method for nine UDDS drive cycles. After 100 iterations, the algorithm terminates and outputs α, i.e., the engine-on power, and β, which equal 12.686 kW and 0.572, respectively. The final output, i.e., the calculated fuel-consumption, is 1.4315 kg. Fig. 11 presents the maximum current, the minimum current, and the engine-on current command, which is proportional to the maximum current. Fig. 12 shows the fuel-consumptions with different methods. When the proposed algorithm is applied, the fuel-consumption is accumulated during the whole trip. The final consumption is 1.395 kg, which is less than the

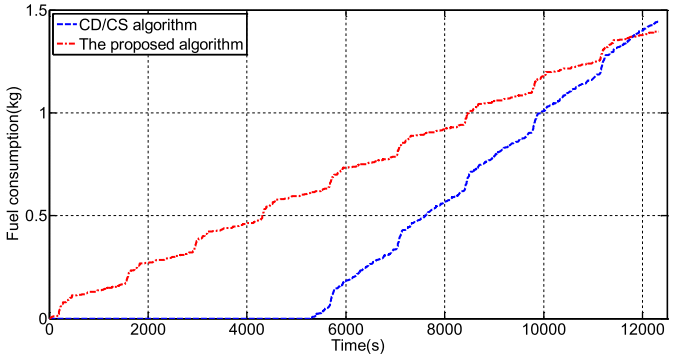

Fig. 12. Fuel-consumption when nine UDDS cycles are simulated with different algorithms.

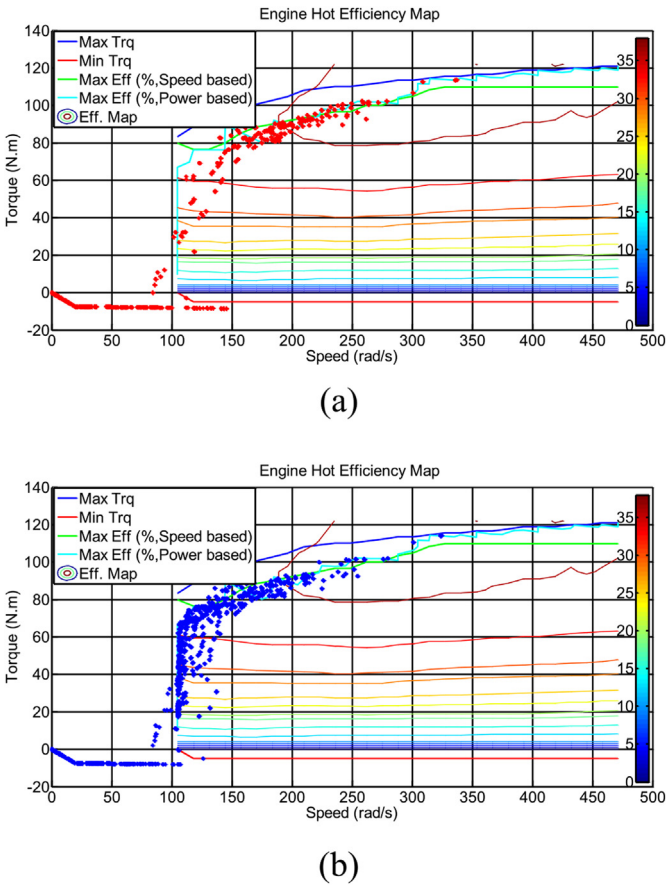

Fig. 13. Engine efficiency comparison when nine UDDS cycles are simulated with different algorithms. (a) The proposed algorithm. (b) CD/CS algorithm.

amount accumulated using the CD/CS method. The simulation result is close to the calculation result in Fig. 10, thereby proving that the quadratic equations are effective in approximating fuel-consumption. Fig. 13 compares the engine efficiency based on different methods; the average engine efficiency is clearly higher when the proposed method is applied. To some degree, this can explain why the proposed method can save fuel-consumption. The calculation was finished within two minutes using a laptop with 2.9 GHz of core i7 processor and 8 gigabits of RAM. From Ref. [18], the computation time for seven UDDS cycles is three minutes. Evidently, the proposed method has a faster calculation speed compared with the method proposed in Ref. [18].

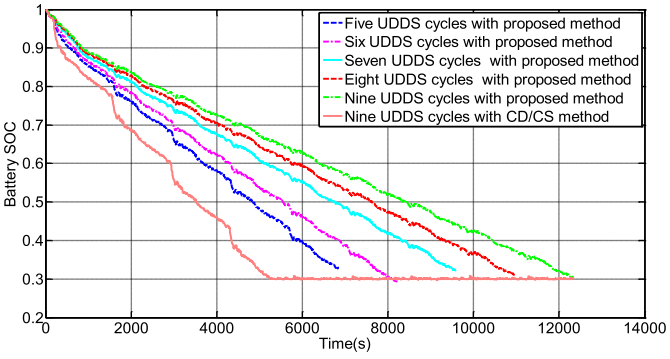

Fig. 14. SoC variation.

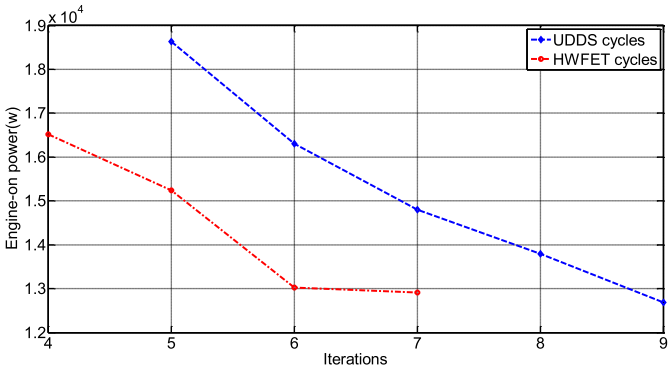

Fig. 15. The computed engine-on power based on the SA method.

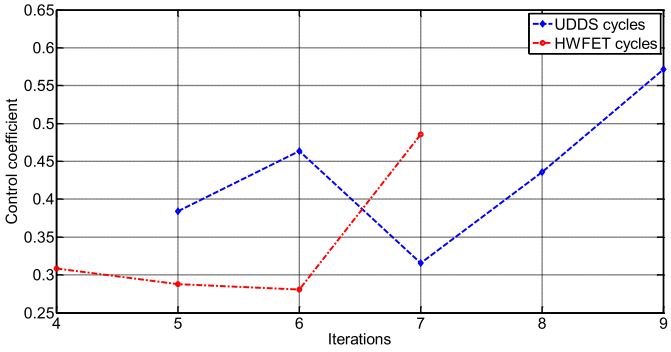

Fig. 16. The calculated current coefficients based on the SA method.

Simulations with five to nine UDDS cycles and four to seven HWFET cycles were carried out with the proposed algorithm. Fig. 14 shows the SoC variations when the vehicle is simulated with five to nine UDDS cycles. The SoC curves all show that the proposed algorithm can gradually discharge the battery to approximately 30% SOC when the trip ends, independent of the driving distances. Fig. 15 depicts the engine-on power calculated by the SA method, which becomes lower as the trip becomes longer. Fig. 16 shows the calculated β, which varies from 0.380 to 0.572. The fuel-consumptions based on different methods are presented in Table 2. In order to calculate the savings, a SoC correction method is applied to make sure the ending SoC values are the same. A linear fitting method is adopted to calculate the SoC correction [8,20,21,29]. Compared with the CD/CS method, the proposed algorithm can save up to 7.24%, 4.81%, 4.59%, 6.26%, and 4.42% of the fuel-consumption when UDDS cycles are simulated and can save up to 9.79%, 4.62%, 5.41%, and 2.91% of the fuel-consumption when HWFET cycles are simulated.

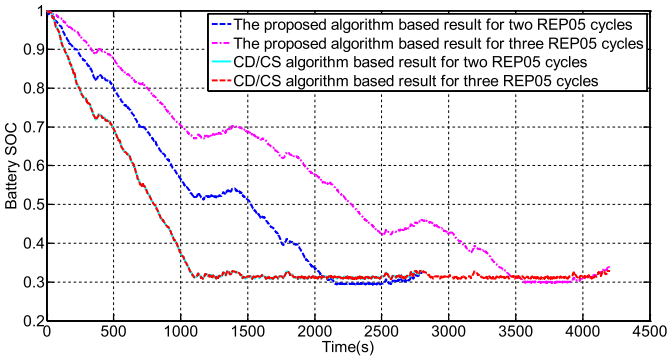

Fig. 17. Battery SoC comparison.

5.2. Simulation with unhealthy battery

To verify the proposed algorithm's robustness, simulations with unhealthy batteries are conducted. REP05 drive cycle is simulated while the battery capacity is 18 Ah, compared with the original capacity of 20 Ah. The vehicle consists of 99 battery cells connected in a series. The average cell OCV is 3.433 V and the average internal resistance is 0.018 Ω. In order to verify the performance of the controller, we separated the simulation into two groups. In Group 1, the internal resistance and battery OCV are assumed unchanged when the battery degrades. In Group 2, each individual cell's OCV drops by 0.1 V and its internal resistance increases by 0.1 Ω. Based on

Table 2
Result comparison.

Drive cycle	Duration (s)	Distance (km)	CD/CS algorithm		The proposed algorithm		Savings (%) (SoC corrected)
			Fuel-consumption (kg)	Ending SoC (%)	Fuel-consumption (kg)	Ending SoC (%)	
5 UDDS	6845	60.35	0.315	30.17	0.344	32.91	7.24
6 UDDS	8214	72.42	0.593	29.79	0.559	29.50	4.81
7 UDDS	9583	84.49	0.877	29.90	0.884	32.40	4.59
8 UDDS	10,952	96.56	1.183	29.81	1.136	31.24	6.26
9 UDDS	12,321	108.63	1.450	30.17	1.395	30.65	4.42
4 HWFET	3060	65.80	0.756	29.93	0.703	31.04	9.79
5 HWFET	3825	82.25	1.200	29.94	1.165	31.02	4.62
6 HWFET	4590	98.70	1.645	29.95	1.576	31.01	5.41
7 HWFET	5355	115.15	2.090	29.94	2.048	31.00	2.97

Table 3
Result comparison.

Group	Drive cycle	CD/CS algorithm		Proposed algorithm		Savings (%) (SoC corrected)
		Fuel-consumption (kg)	Ending SoC (%)	Fuel-consumption (kg)	Ending SoC (%)	
Group 1	2 REP05	1.407	32.81	1.348	32.40	3.64
	3 REP05	2.485	33.90	2.364	33.48	4.55
Group 2	2 REP05	1.504	32.83	1.445	32.38	3.36
	3 REP05	2.676	32.83	2.522	29.34	3.29

the parameters of Group 1, when two REP05 drive cycles are simulated, the engine-on power calculated by the SA method is 25.188 kW and the current coefficient β is 0.071. The fuel-consumptions based on different battery parameters are compared in Table 3. The fuel-consumptions in Group 2 are larger than those in Group 1. This is due to a reduction in battery efficiency caused by a drop in OCV and a rise in internal resistance when the battery is unhealthy. Compared with CD/CS method, the proposed algorithm can save 3.64%, 4.55%, 3.36%, and 3.29% of fuel-consumption when two and three REP05 cycles are simulated. Fig. 17 compares the SoC variations when Group 1 parameters are applied to different methods. It is clear that, with the proposed algorithm, the battery SoC drops more slowly. This proves that even when the battery capacity degrades, the proposed method is still effective in reducing fuel-consumption.

6. Conclusion

In this paper, an energy management strategy based on PMP and the SA method has been proposed to improve the fuel economy of a power-split PHEV. By analyzing the vehicle driveline, the battery current is applied to calculate the fuel-rate with different vehicle driveline powers and speeds. Quadratic equations are employed to describe the relationship between fuel-rate and battery current. By constructing the Hamilton function based on PMP, combinations of the maximum and minimum allowable battery currents are determined to be the optimal solutions for realizing energy management. The SA algorithm is employed to find the engine-on power and the maximum current coefficient. The simulation results show two main contributions of the proposed algorithm: 1) realizing energy management by means of a faster calculation speed; and 2) reducing the fuel-consumption compared with the CD/CS method, independent of trip length. Moreover, the proposed algorithm is still feasible even when the battery SOH changes.

In this paper, the proposed algorithm only focuses on the energy management of a power-split PHEV based on the trip information, and is only verified by simulations. Our next step is to improve energy management for other types of PHEVs, followed by conducting a study focused on experimental validation. In addition, road pattern recognition can also be added to enhance the application of the proposed method.

References

[1] X. Zhang, C. Mi, Vehicle Power Management: Modeling, Control and Optimization, Springer, 2011.
[2] C. Mi, A. Masrur, D.W. Gao, Hybrid Electric Vehicles: Principles and Applications with Practical Perspectives, Wiley, 2011.
[3] C.C. Chan, A. Bouscayrol, K. Chen, IEEE Trans. Veh. Technol. 59 (2010) 589–598.
[4] M. Ehsani, Y. Gao, A. Emadi, Modern Electric, Hybrid Electric, and Fuel Cell Vehicles: Fundamentals, Theory, and Design, second ed., Taylor & Francis, 2009.
[5] C. Zheng, F. Yuhong, C.C. Mi, IEEE Trans. Veh. Technol. 62 (2013) 1020–1030.
[6] J. Gonder, T. Markel, in: Presented at the SAE International, 2007.
[7] M. Koot, J.T.B.A. Kessels, B. de Jager, W.P.M.H. Heemels, P.P.J. Van den Bosch, M. Steinbuch, IEEE Trans. Veh. Technol. 54 (2005) 771–782.
[8] C. Zheng, C.C. Mi, in: Vehicle Power and Propulsion Conference, 2009, VPPC '09, IEEE, 2009, pp. 335–339.
[9] Z. Zhiguang, C. Mi, C. Zheng, A. Masrur, Y.L. Murphey, in: Vehicle Power and Propulsion Conference (VPPC), IEEE, 2011, pp. 1–4.
[10] Z. Zhou, C. Mi, Int. J. Electr. Hybrid Veh. 3 (2011) 246–258.
[11] S. Ebbesen, P. Elbert, L. Guzzella, IEEE Trans. Veh. Technol. 61 (2012) 2893–2900.
[12] S. Stockar, V. Marano, M. Canova, G. Rizzoni, L. Guzzella, IEEE Trans. Veh. Technol. 60 (2011) 2949–2962.
[13] Z. Chen, X. Zhang, C.C. Mi, J. Asian Electr. Veh. 8 (2010) 1425–1432.
[14] S.G. Li, S.M. Sharkh, F.C. Walsh, C.N. Zhang, IEEE Trans. Veh. Technol. 60 (2011) 3571–3585.
[15] Y.L. Murphey, J. Park, Z. Chen, M.L. Kuang, M.A. Masrur, A.M. Phillips, IEEE Trans. Veh. Technol. 61 (2012) 3519–3530.
[16] Y.L. Murphey, J. Park, L. Kiliaris, M.L. Kuang, M.A. Masrur, A.M. Phillips, et al., IEEE Trans. Veh. Technol. 62 (2013) 69–79.
[17] C. Zheng, C.C. Mi, X. Jun, G. Xianzhi, Y. Chenwen, IEEE Trans. Veh. Technol. 63 (2014) 1567–1580.
[18] Z. Chen, C.C. Mi, R. Xiong, J. Xu, C. You, J. Power Sources 248 (2014) 416–426.
[19] H. Borhan, A. Vahidi, A.M. Phillips, M.L. Kuang, I.V. Kolmanovsky, S. Di Cairano, IEEE Trans. Control Syst. Technol. 20 (2012) 593–603.
[20] Z. Menyang, Y. Yan, C.C. Mi, IEEE Trans. Veh. Technol. 61 (2012) 1554–1566.
[21] Z. Bingzhan, C.C. Mi, Z. Mengyang, IEEE Trans. Veh. Technol. 60 (2011) 1516–1525.
[22] Z. Chen, C. Mi, J. Xu, X. Gong, C. You, Online Energy Management for a Power-split Plug-in Hybrid Electric Vehicle Based on Dynamic Programming and Neural Networks, 2013.
[23] M. Ansarey, M. Shariat Panahi, H. Ziarati, M. Mahjoob, J. Power Sources 250 (3/15/2014) 359–371.
[24] G. Qiuming, L. Yaoyu, P. Zhong-Ren, in: IEEE International Conference on Vehicular Electronics and Safety, 2008, ICVES 2008, 2008, pp. 90–95.
[25] P. Jungme, C. Zhihang, L. Kiliaris, M.L. Kuang, M.A. Masrur, A.M. Phillips, et al., IEEE Trans. Veh. Technol. 58 (2009) 4741–4756.
[26] K. Namwook, C. Sukwon, P. Huei, IEEE Trans. Control Syst. Technol. 19 (2011) 1279–1287.
[27] Z. Yuan, L. Teng, S. Fengchun, H. Peng, Energies 6 (2013) 2305–2318.
[28] C. Hou, M. Ouyang, L. Xu, H. Wang, Appl. Energy 115 (2014) 174–189.
[29] P. Pisu, G. Rizzoni, A comparative study of supervisory control strategies for hybrid electric vehicles, Control Syst. Technol., IEEE Trans., 15 (2007) 506–518.
[30] G. Qiuming, L. Yaoyu, P. Zhong-Ren, IEEE Trans. Veh. Technol. 57 (2008) 3393–3401.
[31] A.L. Brooke, Chevrolet Volt: Development Story of the Pioneering Electrified Vehicles, Sae International, 2011.
[32] J.P. Trovão, P.G. Pereirinha, H.M. Jorge, C.H. Antunes, Appl. Energy 105 (2013) 304–318.
[33] S. Hui, Eng. Appl. Artif. Intell. 23 (2010) 27–33.
[34] Z. Chen, C.C. Mi, Y. Fu, J. Xu, X. Gong, J. Power Sources 240 (2013) 184–192.
[35] Wikipedia, Simulated Annealing, Available: http://en.wikipedia.org/wiki/Simulated_annealing#cite_note-1.
[36] M. Harini, J. Adhikari, K.Y. Rani, Ind. Eng. Chem. Res. 52 (2013/05/29) 6869–6893.
[37] N. Kim, M. Duoba, N. Kim, A. Rousseau, SAE Int. J. Passeng. Cars Mech. Syst. 6 (2013) 985–992.
[38] N. Kim, A. Rousseau, E. Rask, Autonomie Model Validation with Test Data for 2010 Toyota Prius, 2012.